 CMC, vol.25, no.1, pp.47-73, 2011

Experimental and Analytical Studies on Concrete Cylinders Wrapped with Fiber Reinforced Polymer

Bhashya V.[1], **Ramesh G.**[1], **Sundar Kumar S.**[1], **Bharatkumar B. H.**[1]
Krishnamoorthy T.S.[1] **and Nagesh R Iyer.**[1]

Abstract: Fibre-reinforced polymers (FRPs) are being introduced into a wide variety of civil engineering applications. These materials have been found to be particularly attractive for applications involving the strengthening and rehabilitation of existing reinforced concrete structures. In this paper, experimental investigations and analytical studies on four series of the concrete cylinders wrapped with FRP are presented. First series consist of concrete cylinders wrapped with one layer carbon fiber reinforced polymer (CFRP), second series concrete cylinders wrapped with two layers CFRP, in third series, concrete cylinders were wrapped with one layer glass fiber reinforced polymer (GFRP) and the fourth series consist of concrete cylinders wrapped with two layers of GFRP.The results show that external confinement significantly improves the ultimate strength and ductility of the specimens.Coupon tests have also been carried out to determine the mechanical properties of the FRP. Further, review of three analytical models for confined concrete from the literature is presented in detail. The stress–strain curve of confined concrete in these models consists of a parabolic first portion and a straightline second portion. Predicted stress-strain curve of these models are compared with authors's experimental curves. In predicting the second portion of the stress-strain curve considerable deviation was observed. An analytical model is also proposed for determining the stress-strain relationship of confined concrete.The model is validated by comparing with experimental values. It is observed that the proposed model well predicts the ultimate axial strains and stresses and reproduce finely the stress–strain response of confined concrete with carbon or glass FRP.

Keywords: FRP, Retrofitting, Analytical models, FRP confined concrete strength, stress-strain curves, FRP coupon.

[1] CSIR – Structural Engineering Research Centre, CSIR Campus, Taramani, Chennai, India.

1 Introduction

Externally applied fiber reinforced polymer (FRP) composites are increasingly being used to strengthen, repair and rehabilitate civil reinforced concrete structures. The reason behind this wide spread popularity can be attributed to its properties such as high strength to weight ratio, ease with which it can be applied at the site and the fact that there is negligible change in the dimension of the structural element. The repair techniques include: column strengthening, seismic applications are using FRP wraps, beam strengthening with bonded FRP wraps and laminates, as well as applications to masonry and other types of structures.

Richart, Brandtzaeg and Brown (1928), Newman and Newman (1972), Mander, Priestly, and Park (1988) have developed stress-strain models to predict the ultimate strength and strain of the confined concrete. These models are developed for steel tube confined concrete columns and were extended to FRP confinement. These models are based on ultimate strength of the concrete. They predict the enhancement of the confined concrete as a function of the confining pressure. Fardis and Khalili (1982) reviewed the empirical formula by Richart, Brandtzaeg and Brown (1928) to quantify the increase in the concrete compressive strength and the nonlinear expression by Newman and Newman (1972) to obtain an equation to predict the confined concrete strength by substituting the maximum confining pressure that FRP can exert. It was observed that these steel-based confinement models over estimated the effectiveness of the confining pressure.

Nanni and Bradford (1995) conducted experiments on 150 x 300 mm cylinders, which were confined laterally, spirally with different FRP composites. It was observed that the confined concrete with FRP enhanced strength and pseudo-ductility of the concrete. A comparison of the prediction by two existing models Mander, Priestly, and Park (1988), Fardis and Khalili (1982) was conducted. The studies concluded that the models proved to be sufficiently accurate for prediction of the strength, but underestimated the ultimate strain of concrete confined with FRP materials. It was also observed that the passive FRP confinement did not prove advantageous under load conditions below the unconfined concrete strength. Mirmiran and Shahawy (1996) developed a concrete filled hollow FRP composite column which was similar to the classic concrete filled steel tubes. Behavior of the model was proposed by developing a new passive confinement model for externally reinforced concrete columns with a composite action model that evaluates the lateral stiffening effect of the jacket. The studies concluded that the degree of composite action was appropriately defined as a function of bond strength of the material. Karbhari and Gao (1997) also developed experimental data based on variety of reinforcing fiber types, orientations and jacket thickness and sugested simple design equations to estimate the response of composite confined concrete. They concluded

that development of a true composite model was required rather than empirical models which include effects of both the fiber reinforced composite and the concrete on a true material basis. Their model attempted to address the deficiencies, from the aspect of composite materials modeling, but fell short of modeling the true response of the composite that changes as the stress level increases. In this paper, tensile test on FRP coupons was carried out to determine the mechanical properties of the FRP. Experimental investigations have been carried out to study the behaviour of FRP confined concrete. Further, review of three analytical models for confined concrete from the literature is presented in detail. Predicted stress-strain curve of these models are compared with authors's experimental curves. And also, an analytical model is proposed for determining the stress-strain relationship of confined concrete.The model is validated by comparing with author's experimental values.

2 Experimental Investigations

2.1 Tensile Test on FRP Coupons

General guidelines specified in ASTM D3039-08 were followed while testing the FRP coupons. A 25 mm width for the coupons were kept constant for both glass and carbon fibre, when the length of carbon fibre was 250 mm and that of glass fibre 300 mm. CFRP laminates were provided as tabs at both the ends to prevent premature failure at the grips. The tabs were chamfered at 45 degree to avoid any stress concentration. The fibres were smear with a thin layer of epoxy on both sides and allowed to cure in air for one day. For coupons with two layers of fibre the second layer of the fibre was pasted immediately after the epoxy was pasted on the first layer when the epoxy was still wet. The subsequent day the coupons were cut for the required dimension and the tabs pasted (Fig. 1).

The coupons were further allowed to cure for seven days before testing. Electrical strain gauge of 2 mm gauge length was pasted on the coupons before testing. The coupons were tested in a 500 kN servo controlled universal testing machine (Fig. 2).

Flat grips were used to grip the specimens at a grip-pressure of 3.5 N/mm^2. The load was applied at a rate of 1mm/min till failure. Fig.3 shows the typical stress-strain plots of the coupons.

It was observed that the stress-strain curve of FRP cupons was linear up-to failure load. Elastic modulus of CFRP and GFRP are 208 GPa, 75 Gpa, respectively. The maximum strain at failure was well beyond 0.012. Where as the failure stress were around 2500 MPa for the carbon fibre and 830 MPa for glass fibre. **Fig. 4** shows few typical failure patterns of the coupons. The failures of the coupons were due to

Figure 1: FRP Coupons with Tabs

Figure 2: Testing of FRP Coupon in 500 kN Servo Hydraulic UTM

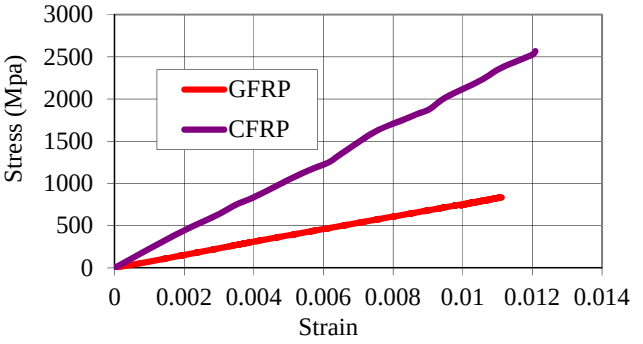

Figure 3: Typical stress-strain plot for FRP coupons

a) Glass fibre b) Carbon fiber

Figure 4: Typical failure pattern of FRP coupons

the rupture of the fibre.

2.2 Compression Test on FRP Confined Concrete Cylinders

Cylinders of 150 mm diameter and 300 mm height were cast and cured under water for 28 days. The 28 days average compressive strength of the cylinders was 47 MPa. The cylinders were dried after removing from water for one day. The surface of the cylinder was roughened with powered wire brush (Fig. 5) and cleaned with air under pressure to remove the loose particles.

A primer coat was applied and allowed to dry for one day. A two component epoxy system was prepared as per the manufacturer's recommended procedure, a thin layer of epoxy was applied on the cylinder surface and the fibre fabric was wrapped around the cylinder, subsequently a second layer of epoxy was applied

Figure 5: Surface Preparation of Cylinders with Wire Brush

on the fibre fabric. For specimens to be strengthened with two layers of fibre, the second layer was wrapped when the epoxy was still wet and then it was coated with another layer of epoxy. The orientation of the fibers in case of CFRP was in the hoop direction, in case of GFRP since the fibre mat itself is bi-directional the fibre distribution was equal in both the direction. The strengthened specimens were air cured for seven days before testing. Fig. 6 shows a cylinder being wrapped with carbon fibre.

The top and the bottom surface of the cylinders were smoothened with the help of grinding machine and subsequently capped with sulphur to obtain a truly horizontal surface. Fig. 7 shows the capped specimens.

The testing was done in a 2500 kN servo controlled UTM. Two LVDT's were place diametrically opposite to measure the displacement. The displacement was measured between the two platens.Electrical strain gauges of gauge length 2 mm were pasted on FRP to measure the strain. The strain gauges and the LVDT's were connected to an online data acquisition system. The cylinder was placed concentrically in the testing matching. Fig. 8 shows a typical view of testing in progress.

In the present investigation, four set of the concrete cylinders wrapped with FRP are presented. First set consist of concrete cylinders wrapped with single layer carbon fiber reinforced polymer (CFRP), second, concrete cylinders wrapped with two layers CFRP, third, concrete cylinders wrapped with single layer GFRP and the fourth set consist of concrete cylinders wrapped with two layers of glass fiber reinforced polymer (GFRP). 3 unconfined concrete specimens were tested and for each

Figure 6: Wrapping of Cylinder with Carbon Fibre

Figure 7: Capped Specimens

set 3 specimens were tested. **Fig.9** shows the stress-strain curve of FRP strengthen concrete cylinders.

From the results it was clear that the addition of second layer of the fibre increase the peak load by around 30 percent for carbon fibre and by 40 percent for glass

Figure 8: Typical View of Testing of the Cylinders

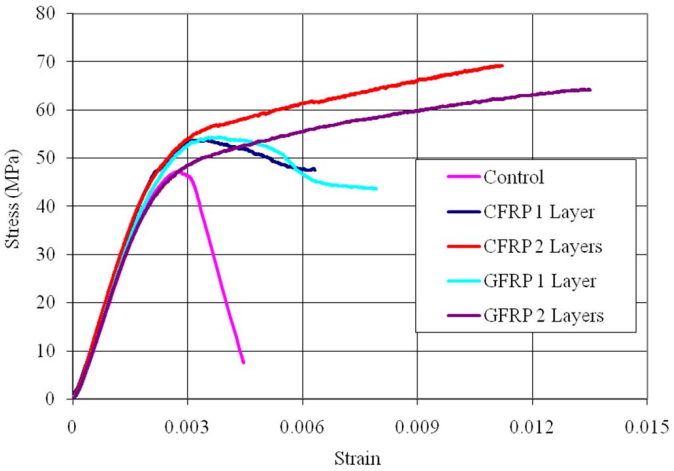

Figure 9: Typical stress-strain curves of FRP strengthened concrete cylinders

fibre when compared to the control specimens, whereas with one layer of fibre, the load increase was around 10 -11 percent for both carbon as well as glass fibre. **Fig. 10** shows the failure patterns of the various cylinders.

All the confined cylinders failed due to the rupture of the fibers indicating a good bond between the concrete and the fibre-epoxy system. The failure was sudden and violent with a loud sound for carbon fibre strengthened specimens, whereas


10.1 Control Specimens




10.2 (a) One Layer Carbon Fibre 10.2 (b) Two Layer Carbon Fibre




10.3 (a) One Layer Glass Fibre 10.3 (b) Two Layer Glass Fibre

Figure 10: Failure Patterns for concrete cylinders wrapped with FRP

for the glass fibre specimens though the failure was sudden it was not violent. The summary of the test results of the cylinders are given in Table 1.

3 Review of Fiber-Reinforced Polymer-Confinement Models

The three analytical model presented are model proposed by Toutanji (1999), Berthet, Ferrier and Hamelin (2006) and Lam and Teng (2003).

3.1 Model proposed by Toutanji (1999)

Toutanji (1999) proposed a model to predict the stress-strain curves of concrete externally confined with FRP sheets. This model calculates the second branch of

Table 1: Test Results for Cylinders

Specimen Id	Compressive Strength(MPa)	Axial Strain at Peak load	% Increase in Compressive Strength
Control	47.30	0.0028	-
CSL	53.60	0.0032	13.31
CDL	69.13	0.0112	46.15
GSL	54.22	0.0040	14.63
GDL	63.88	0.0130	35.05

CSL – Carbon Single Layer, CDL – Carbon Double Layer, GSL – Glass Single Layer, GDL – Glass Double Layer

the stress-strain diagram first. Then the equations for the first branch are provided based on an equation proposed by Ahmad and Shah (1982). Finally, the transition point is determined which indicates when the equations for stress and strain and the values for first branch become invalid, and when the equations for stress and strain and the values for the second branch become valid. The experimental data is then compared with the predicted stress and strain values from the model.

With the assumption that the deformation in the concrete and the FRP confinement are compatible and will produce the same strains, **Fig.11** is the free-body diagram demonstrating how the lateral stress will be calculated.

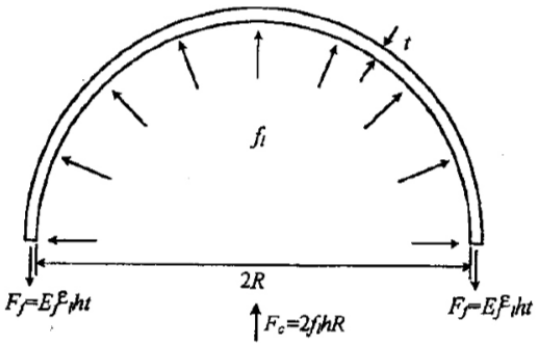

Figure 11: Cross section of confinement and mechanics produced by FRP

Based on the equilibrium equations and the deformation compatibility assumption, the lateral stress can be calculated using Equation 1

$$f_l = E_l \varepsilon_l \tag{1}$$

Where E_l = lateral elastic modulus and ε_l = lateral strain of the confined specimens. Where E_l is calculated using Equation 2, which represents the stiffness of the confinement,

$$E_l = \frac{E_{frp}t}{R} \tag{2}$$

Where E_{frp} = elastic modulus of the FRP as provided by the manufacturer, t = thickness of the FRP, and R = radius of the cylinder. Since the elastic modulus of the epoxy is small in comparison to that of the FRP, it is not considered necessary in calculating the lateral elastic modulus (E_l) of the confined specimens.

For the development of the second branch, Equation 4 was modified from Equation 3. Equation 3 was used by Richart, Brandtzaeg and Brown (1928) to calculate the ultimate confining stress based on concrete laterally confined with hydrostatic pressure and spiral reinforcement.

$$f_{cc} = f'c + k_1\, f'_l \tag{3}$$

Where f_{cc}= confined concrete strength, $f'c$ = ultimate unconfined concrete stress, k_1 = confinement effectiveness coefficient and f'_l = lateral pressure. Richart et al assumed k_1 to be constant at 4.1 while others believe it to vary between 4.5 and 7.0 with an average value of 5.6. Equation 4 is as follows

$$f_a = f'c + k_1\, f_l \tag{4}$$

Where f_a = calculated axial stress and f_l = lateral stress applied to the concrete by the FRP. For this model, values for k_1 were plotted at a function of the ratio between lateral stress and concrete strength $\left(\frac{f_l}{f'c}\right)$, with the use of a regression analysis, an equation for k_1 was determined with a coefficient of determination of 0.80.

$$k_1 = 3.5\left(\frac{f_l}{f'c}\right)^{-0.15} \tag{5}$$

Substituting Equation 5 into Equation 4 will result in Equation 6. This equation will be used to calculate the stress for every point along the second branch of the stress-strain diagram.

$$f_a = f'c\left[1 + 3.5\left(\frac{f_l}{f'c}\right)^{0.85}\right] \tag{6}$$

Richart, Brandtzaeg and Brown (1928) demonstrated that the axial strain at the maximum stress increases as a function of the lateral pressure. This is shown in Equation 7,

$$\varepsilon_{ca} = \varepsilon_0\left[1 + 5k_1\left(\frac{f'_l}{f'c}\right)\right] \tag{7}$$

Where ε_{ca} = axial strain in strength of confined concrete. If the equations used by Richart, Brandtzaeg and Brown (1928) are substituted into the equations and simplified, the axial strain for the second branch can be calculated by using

$$\varepsilon_a = \varepsilon_0 \left[1 + k_2 \left(\frac{f_a}{f'c} - 1 \right) \right] \tag{8}$$

Where ε_a = axial strain of specimens, k_2 = concrete strain enhancement coefficient and can be calculated with Equation 9, which was determined using a regression line and plotted as a function of the lateral strain with a coefficient of determination of approximately 0.85.

$$k_2 = 310.57\varepsilon_l + 1.9 \tag{9}$$

Combining Equation 9 with Equation 8 will result in one last combination and simplification, resulting in the final equation (Equation 10) for determining the axial strain corresponding to the stress for the second portion of the stress-strain diagram.

$$\varepsilon_a = \varepsilon_0 \left[1 + (310.57\varepsilon_l + 1.9) \left(\frac{f_a}{f'c} - 1 \right) \right] \tag{10}$$

For the creation of the first branch of the stress-strain diagram, an equation, first proposed by Sargin (Toutanji, 1999) for unconfined concrete and modified by Ahmad and Shah (1982), was again modified by Toutanji (1999). Equation 11 was proposed to calculate the stress of the stress-strain diagram based on a given set of boundary conditions when the stress equals zero and the first and second branches intersect.

$$f_a = \frac{A\varepsilon}{1 + B\varepsilon + C\varepsilon^2} \tag{11}$$

where the values for the coefficients can be determined from the equations below.

$$A = E_{ia} \tag{12}$$

$$B = \frac{\mathrm{E_{ia}}}{f_{ua}} - \frac{2}{\varepsilon_{ua}} + \frac{E_{ua}\, E_{ia} \varepsilon_{ua}}{f_{ua^2}} \tag{13}$$

$$C = \frac{1}{\varepsilon_{ua^2}} - \frac{E_{ua}\, E_{ia}}{f_{ua^2}} \tag{14}$$

where E_{ia}= initial tangent of modulus of elasticity of $f_a - \varepsilon_a$curve, f_{ua} = axial stress between elastic and plastic regions, ε_{ua} = strain between the elastic and plastic regions in the axial direction, and E_{ua} = tangent of modulus of elasticity between

elastic and plastic regions of $f_a - \varepsilon_a$ curve. When the stress is zero, the value of E_{ia} is assumed to equal that of plain, unconfined concrete because the FRP is not engaged at this stress. Equation 15 through Equation 18 will be used to calculate the boundary constants *A*–*C*. These constants are determined using Equation 12 through Equation 14 and are used in determining the stress in Equation 11. However, these equations must be used with values in MPa. When substituted into Equation 11, the change between the first branch and the second branch smoothly transition due to the equations below.

$$\mathrm{E_{ia}} = 10200\left(f'_{\mathrm{c}}\right)^{\frac{1}{3}} \tag{15}$$

$$f_{ua} = f'_c \left[1 + 0.0178\left(\frac{E_l}{f'c}\right)^{0.85}\right] \tag{16}$$

$$\varepsilon_{ua} = \varepsilon_0 \left[1 + 0.0448\left(\frac{E_l}{f'c}\right)^{0.85}\right] \tag{17}$$

$$E_{ua} = 0.3075\frac{f'c}{\varepsilon_0} \tag{18}$$

Combining the above-mentioned equations for the first and second branches with values in MPa will result in the stress-strain diagram.This model's predicted stress and strain values will be compared with the actual test data.

3.2 Model proposed by Berthet, Ferrier and Hamelin (2006)

The model proposed by Berthet, Ferrier and Hamelin (2006) first predicts the ultimate stress and ultimate strain of concreted confined by externally applied composite jackets. This model is based on an equation proposed by Toutanji (1999) which is used to calculate the stress in the first branch. The expected ultimate stress is used to calculate the transition point between the first and second branch. Then, an axial strain corresponding to the radial strain of 0.002 was calculated. Once the transition strain and stress are calculated, the second branch can be determined from the stress and strain equal to and greater than that of the transition stress and strain values. The stress for the first branch is then calculated and displayed with the corresponding strain up to the transition stress and strain.

The ultimate strength of the confined concrete (f'_{cc}) is assessed with the relation (19) in function of unconfined ultimate concrete strength (f'_{c0}) and ultimate confinement pressure (f_{lu}), obtained by a regression analysis.

$$f'_{cc} = f'_{c0} + k_1\, f_{lu} \tag{19}$$

where f'_{cc} = ultimate confined concrete strength, f'_{c0} = ultimate unconfined compressive concrete strength, k_1 = efficiency ratio and was determined with regression analysis to be a constant of 3.45 when the unconfined compressive strength is between about 20MPa and 50MPa, while k_1 was a function of the unconfined compressive strength, calculated by Equation 20, if the unconfined compressive strength was greater than about 50MPa up to about 200MPa and f_{lu} = ultimate confinement pressure.

$$k_1 = \frac{9.5}{f'^{\frac{1}{4}}_{c0}} \tag{20}$$

To determine the ultimate confinement pressure, the equilibrium equations for the cross section of an FRP-confined specimen were used under the assumption of compatibility between the concrete core and the FRP. The lateral confining stress can be determined by using and Equation 21.

$$f_l = \frac{t}{r} E_{frp} \varepsilon_r \tag{21}$$

where f_l = lateral confining stress, t and r are the thickness of the FRP and radius of the concrete core, respectively, E_{frp} = modulus of elasticity of the FRP as provided by the manufacturer, ε_r = radial strain. Since the ultimate confining stress is needed to calculate the ultimate confined stress, Equation 22 is a modification of Equation 21 in which the ultimate strain in the FRP jacket is used as provided by the manufacturer;

$$f_{lu} = \frac{t}{r} E_{frp} \varepsilon_{fu} \tag{22}$$

where f_{lu} = ultimate lateral confining stress, ε_{fu} = ultimate radial strain as provided by the manufacturer and all other variables remain the same. Substituting Equation 22 into Equation 19 with the appropriate k_1 value will result in Equation 23.

$$f'_{cc} = f'_{c0} + k_1 \frac{t}{r} E_{frp} \varepsilon_{fu} \tag{23}$$

To define the ultimate strain, the relationship between the confining pressure and the transverse strain must be defined as in Equation 23, along with the expression for the strain ratio shown below in Equation 24;

$$E_l = \frac{\partial f_l}{\partial \varepsilon_r} = \frac{t}{r} E_{frp}$$

$$\gamma = \frac{1}{\sqrt{2}} \left(\frac{E_l}{f'^{2}_{c0}} \right)^{-\frac{2}{3}} \tag{24}$$

where E_l = confinement modulus of elasticity, ∂f_l = change in confining stress, $\partial \varepsilon_r$ = change in radial strain, t and r are the thickness of the FRP and the radius of the concrete core, respectively, E_{frp} = Young's modulus of confinement of the FRP, γ = plastic strain ratio, and f'_{c0} = unconfined compressive strength of concrete. With the above equations defined, the ultimate strain can now be calculated using Equation 25

$$\varepsilon_{au} = \varepsilon_{a0} + \sqrt{2}\left(\frac{E_l}{f'_{c0^2}}\right)^{\frac{2}{3}} (\varepsilon_{fu} - v_c \varepsilon_{a0}) \tag{25}$$

where ε_{au} = ultimate axial strain of confined concrete, ε_{a0} = ultimate axial strain of unconfined concrete (typically taken to be 0.002 inch/inch), ε_{fu} = ultimate FRP strain as provided by the manufacturer, and v_c = Poison's ratio (typically taken to be 0.2). Plotting the ultimate stress and ultimate strain should result in a single point with which the second branch should end. The second branch of the stress-strain diagram for confined concrete is linear. For calculating the second branch, the slope of this linear relationship was determined with a best fit linear regression with a 99% coefficient of determination to be determined by using Equation 26

$$\theta_r = 2.73E_l - 163 \tag{26}$$

where θ_r = slope of the pseudo-plastic branch which corresponds to the change in stress with the change in plastic strain. Since this model is constructed from end to beginning, the slope of the line for the second branch as calculated by Equation 26 will be used to determine the intersection

point for the first and second branches. Now that the slope is defined, the transition point must be defined. The transition point is where the second branch will smoothly join together the first and second branches of the stress-strain diagram. First, the transition stress value will be calculated using Equation 27

$$f'_{cp} = f'_{cc} - \theta_r (\varepsilon_{fu} - \varepsilon_{rp}) \tag{27}$$

where f'_{cp}= reference plastic stress or the transition stress where the first and second branch intersect and ε_{rp} = radial strain at the intersection between the first and second branch; this value will be taken as 0.002 inch/inch. Then, the transition stress is used with Equation 28

$$f'_c = f'_{cp} + \theta_r (\varepsilon_r - \varepsilon_{rp}) \tag{28}$$

where $\varepsilon_r \geq \varepsilon_{rp}$ so that every value of stress for the second branch can be calculated for every value of radial strain greater than that of ε_{rp}. Establishing a connection

between the radial strain and the axial strain will allow for the equations above to be applied when the axial strain is known. The relationships are as follows:

$$\varepsilon_r = v_c \varepsilon_a \tag{29}$$

$$\varepsilon_r = v_c \varepsilon_{a0} + \gamma(\varepsilon_a - \varepsilon_{a0}) \tag{30}$$

where Equation 29 would be used when $\varepsilon_a \leq \varepsilon_{a0}$ and Equation 30 would be for when $\varepsilon_a \geq \varepsilon_{a0}$ and where Equation 24, above, would define γ. With the equations above, the stress corresponding to the axial strain can be determined with a few simple substitutions. This will result in Equation 31

$$f'_c = f'_{cp} + \theta_r [(v_c - \gamma)\varepsilon_{a0} - \varepsilon_{rp}] + \theta_r \gamma \varepsilon_a \tag{31}$$

when $\varepsilon_a \geq \varepsilon_{ap}$ where ε_{ap} is found using Equation 32

$$\varepsilon_{ap} = \varepsilon_{a0} + \frac{\varepsilon_{rp} - \varepsilon_{r0}}{\gamma} \tag{32}$$

where ε_{ap} = axial plastic strain corresponding to ε_{rp}, ε_{a0} = unconfined compressive strain (typically 0.002), and ε_{r0} = radial strain of unconfined concrete which can be determined using Poisson's ratio (assuming that the value for Poisson's ratio is 0.2 as is customarily agreed upon as standard) and ε_{a0}.

$$f'_c(\varepsilon) = \frac{A\varepsilon}{1 + B\varepsilon + C\varepsilon^2} \tag{33}$$

where the coefficients A, B, and C can be determined by Equation 34, Equation 35, and Equation 36 and where E^*_r represents the transverse equivalent modulus of the multimaterial of the FRP and the concrete core, which can be determined using Equation 37.

$$A = E^*_r \tag{34}$$

$$B = \frac{E^*_r}{f'_{cp}} - \frac{2}{\varepsilon_{rp}} + \theta_r \frac{E^*_r \varepsilon_{rp}}{f_{cp^2}} \tag{35}$$

$$C = \frac{1}{\varepsilon_{rp}} - \theta_r \frac{E^*_r}{f'_{cp^2}} \tag{36}$$

$$E^*_r = \frac{E_c}{v_c}\left[1 + \frac{E_l}{E_c}(1 - v_c)\right] \tag{37}$$

For Equation 33 to be used with axial strains instead of radial strains, there must be an alteration where ε is replaced by ε_a. This will result in changed boundary

conditions and a slight change in the coefficients defined above, where $E^*{}_r$ will be replaced with $E^*{}_a$ which is defined as Equation 38

$$E^*{}_a = E_c \frac{E_c + (1 - v_c) E_l}{E_c + \left(1 - v_c - 2{v_c}^2\right) E_l} \tag{38}$$

where $E^*{}_a$ represents the equivalent elastic modulus. The equation above, in conjunction with the translation between the axial strain corresponding to the radial strain ε_{rp}, can be used to substitute into Equation 33, which will result in Equation 39.

$$f'_c = \frac{E^*{}_a \varepsilon_a}{1 + \left(\frac{E^*{}_a}{f'_{cp}} - \frac{2}{\varepsilon_{ap}} + \theta_r \frac{E^*{}_a \varepsilon_{ap}}{f_{cp^2}}\right) \varepsilon_a + \left(\frac{1}{{\varepsilon_{ap}}^2} - \theta_r \frac{E^*{}_a}{{f'_{cp}}^2}\right) {\varepsilon_a}^2} \tag{39}$$

Combining the stress values from Equation 39 partnered with the axial strain up to ε_{ap} along with the stress values obtained from Equation 31 together with the strains greater than ε_{ap} will result in the complete stress-strain diagram.

3.3 Model proposed by Lam and Teng (2003)

Lam and Teng (2003) compare the results from design-oriented models and analysis-oriented models. They then propose a design-oriented model compiled by test data from open literature based on the four parameters by Richard and Abbot (1975). The use of analysis-oriented models to help with the correlation between the FRP jacket stiffness and that of the concrete assisted in the prediction of the ultimate confined strain. This model uses simple equations breaking up the first and second branch, with two equations at a transition strain based on the modulus of elasticity of second branch based on the ultimate confined stress, the reference stress and the ultimate strain. The basic assumptions of this simple model are: (i) the stress–strain curve consists of a parabolic first portion and a straight line second portion. (ii) the slope of the parabola at $\varepsilon_c = 0$ (initial slope) is the same as the elastic modulus of unconfined concrete E_c; (iii) the nonlinear part of the first portion is affected to some degree by the presence of an FRP jacket; (iv) the parabolic first portion meets the linear second portion smoothly (i.e. there is no change in slope between the two portions where they meet); (v) the linear second portion ends at a point where both the compressive strength and the ultimate axial strain of confined concrete are reached.

Based on the assumptions listed above, the stress–strain model for FRP-confined concrete is given by the following expressions:

$$\sigma_c = E_c \varepsilon_c - \frac{(E_c - E_2)^2}{4 f'_{c0}} {\varepsilon^2}_c \text{ for } 0 \leq \varepsilon_c \leq \varepsilon_t \tag{40}$$

and

$$\sigma_c = f'_{c0} + E_2\varepsilon_c \text{ for } \varepsilon_t \leq \varepsilon_c \leq \varepsilon_{cu} \tag{41}$$

where f'_{c0}=intercept of the stress axis by the linear second portion. The parabolic first portion meets the linear second portion with a smooth transition at ε_t, which is given by

$$\varepsilon_t = \frac{2f'_{c0}}{E_c - E_2} \tag{42}$$

where f'_{c0}, E_c are the compressive strength, elastic modulus of unconfined concrete and E_2 is the slope of the linear second portion, given by

$$E_2 = \frac{f'_{cc} - f'_{c0}}{\varepsilon_{cu}} \tag{43}$$

Where f'_{cc} compressive strength of confined concrete.

The compressive strength f'_{cc} and ultimate axial strain ε_{cu} of FRP- confined concrete are defined by:

$$\frac{f'_{cc}}{f'_{c0}} = 1 + 3.3\frac{f'_l}{f'_{c0}} \tag{44}$$

and

$$\frac{\varepsilon_{cu}}{\varepsilon_{c0}} = 1.75 + 12\frac{f'_l}{f'_{c0}}\left(\frac{\varepsilon_{h,rup}}{\varepsilon_{c0}}\right) \tag{45}$$

actual maximum confining pressure is given by

$$f_l = \frac{E_{frp}t\varepsilon_{h,rup}}{\mathrm{R}} \tag{46}$$

3.4 Proposed model

Error in prediction of stress-strain curve of FRP confined concrete cylinders using the above models is quite high. Therefore the model proposed by Lam and Teng (2003) was modified to accurately predict the stress-strain resposnce of confined concrete cylinders. Concrete cylinders wrapped with single layer carbon/glass fibers shows a parabolic first portion and a linear post-peak descending branch, where as those cylinders wrapped with two layers of carbon/glass fibers shows a parabolic first portion and linear ascending branch later.

The ratio of the confinement modulus ($\frac{E_{frp}t}{R}$) to the square of unconfined concrete strength $(f'_{co})^2$ for concrete cylinders wrapped with single layer carbon and double layer carbon are 0.147 (Mpa^{-1}), 0.294 (Mpa^{-1}) respectively and those cylinders wrapped with single layer glass and double layer glass are 0.154 (Mpa^{-1}), 0.308 (Mpa^{-1}), respectively. Xiao and Wu (2000) suggested that the ratio of the confinement modulus to the square of unconfined concrete strength $(f'_{co})^2$ less than 0.2 (Mpa^{-1}), a post-peak descending branch could be expected. This trend was also observed in the experiments carried out during this study. Therefore the term $\frac{C}{(f'_{co})^2}$ is used as limits to decide wether the linear second portion of the curve descending or ascending branch. Where the confinement modulus (C) is given by $C = \frac{E_{frp}t}{R}$

The stress–strain model for FRP-confined concrete is given by the following expressions:

$$\sigma_c = E_c\varepsilon_c - \frac{(E_c - E_2)^2}{4f'_{c0}}\varepsilon^2{}_c \text{ for } 0 \le \varepsilon_c \le \varepsilon_t \tag{47}$$

$$\sigma_c = f'_{c0} + E_2\,(1.3\varepsilon_{cu} - \varepsilon_c) \text{ for } \varepsilon_t \le \varepsilon_c \le \varepsilon_{cu} \text{ and } \frac{C}{(f'_{co})^2} < 0.2 \tag{48}$$

$$\sigma_c = f'_{c0} + E_2\varepsilon_c \text{ for } \varepsilon_t \le \varepsilon_c \le \varepsilon_{cu} \text{ and } \frac{C}{(f'_{co})^2} > 0.2 \tag{49}$$

Where, f'_{c0}=Compressive strength of unconfined concrete. Based on regression analysis of extensive experimental data, a factor of 1.3 (Eq.48) has been arrived to take care of softening region. The parabolic first portion meets the linear second portion with a smooth transition at ε_t, which is given by

$$\varepsilon_t = \frac{2f'_{c0}}{E_c - E_2} \tag{50}$$

where f'_{c0} and E_c are the compressive strength and elastic modulus of unconfined concrete respectively; and E_2 is the slope of the linear second portion, given by

$$E_2 = \frac{f'_{cc} - f'_{c0}}{\varepsilon_{cu}} \tag{51}$$

Where f'_{cc} compressive strength of confined concrete.

Compressive strength (f'_{cc}) of FRP confined concrete proposed by Karbari and Gao (1997) given in equation 52 has been used.

$$f'_{cc} = f'_{c0} + 2.1f'_{c0}\left(\frac{2f_{com}t}{df'_{c0}}\right)^{0.87} \tag{52}$$

Where f'_{c0}= Compressive strength of unconfined concrete, t =thickness of FRP, f_{com}= tensile strength of FRP, d = diameter of concrete cylinder

Ultimate axial strain (ε_{cu}) of FRP confined concrete proposed by Cusson and Paultre (1995) given in equation 53 has been used.

$$\varepsilon_{cu} = \varepsilon_{c0} + 0.21\left(\frac{f_l}{f'_{c0}}\right)^{1.7} \tag{53}$$

Where confining pressure given by $f_l = \frac{2f_{com}t}{d}$

ε_{c0}=Ultimate axial strain of unconfined concrete, ε_{cu}= Ultimate axial strain of confined concrete

Stress-strain curve for FRP confined concrete using proposed model will be obtained using equations 47, 48 and 49.

Predicted values of the ultimate strain and compressive strength of the concrete cylinders confined with CFRP using the model proposed by Toutanji (1999), Lam and Teng (2003), Berthet, Ferrier and Hamelin (2006) and proposed model are presented in Table 2 and those cylinders confined with GFRP are presented in Table 3.

Input values of these models for CFRP are given in Table 4 and those values for GFRP are given in Table 5.

Fig.12 shows the comparison of predicted stress-strain curves by all the models (Toutanji (1999), Lam and Teng (2003), Berthet, Ferrier and Hamelin (2006) and Proposed model) with the actual test data.

In the model proposed by Toutanji (1999), a bilinear relationship for stresses and strains is determined for FRP-confined concrete cylinders. From Fig.12 it can be seen that the initial stiffness of the stress-strain curve is slightly higher compared to experimental curve. From **Table 2** and **3** it is observed that, error in prediction of compressive strength of concrete cylinders confined by carbon fiber was 24% for single layer and 27% for double layer. In case of cylinders wrapped with single layer glass fiber error in prediction of ultimate stress was 22% and for double layer it was 10%.

In the design-oriented model proposed by Lam and Teng (2003), the effect due to the stiffness of the FRP jacket is added as a parameter that controls the initial shape of the stress-strain diagram.The comparison of the predicted stress-strain curve by Lam and Teng with the actual test data given in **Fig 12**.

Berthet, Ferrier and Hamelin (2006) model constructs a bilinear relationship for FRP-confined concrete, predicting the ultimate stress and strain, then the second branch of the stress-strain diagram followed by the first branch. From **Table 2**

Table 2: Predicted values of the compressive strength and ultimate strain of concrete cylinders confined with CFRP

S.No	Ultimate strain Model (ε)	Ultimate strain Exp (ε_{exp})	$\varepsilon/\varepsilon_{exp}$	Comp strength Model (fcc) Mpa	Comp strength Exp (fcc $_{exp}$) Mpa	fcc/fcc $_{exp}$
Carbon single layer						
Toutanji(1999)	0.0068	0.0063	1.079365	66.86	53.60	1.247442
Lam&Teng (2003)	0.0056		0.888889	59.89		1.11747
Berthet,Ferrier, Hamelin (2006)	0.0065		1.031746	60.30		1.125097
Proposed model	0.0051		0.809524	54.01		1.007649
Carbon double layer						
Toutanji (1999)	0.0129	0.0112	1.151786	87.81	69.13	1.270292
Lam&Teng (2003)	0.0087		0.776786	77.30		1.118276
Berthet,Ferrier, Hamelin (2006)	0.0100		0.892857	75.51		1.092371
Proposed model	0.0121		1.080357	67.87		0.981844

Table 3: Predicted values of the compressive strength and ultimate strain of concrete cylinders confined with GFRP

S.No	Ultimate strain Model (ε)	Ultimate strain Exp (ε_{exp})	$\varepsilon/\varepsilon_{exp}$	Comp strength Model (fcc) Mpa	Comp strength Exp (fcc $_{exp}$) Mpa	fcc/fcc $_{exp}$
Glass single layer						
Toutanji (1999)	0.0064	0.0079	0.810127	66.2396	54.22	1.221682
Lam&Teng (2003)	0.0054		0.683544	59.4216		1.095935
Berthet,Ferrier, Hamelin (2006)	0.0063		0.797468	59.9862		1.106348
Proposed model	0.0053		0.670886	54.49		1.004978
Glass double layer						
Toutanji (1999)	0.0054	0.013	0.415385	70.3003	63.88	1.100506
Lam&Teng (2003)	0.0078		0.6	73.7450		1.15443
Berthet,Ferrier, Hamelin (2006)	0.0096		0.738462	75.8057		1.186689
Proposed model	0.0124		0.953846	68.2336		1.068153

Table 4: Input data used in the models for carbon fiber reinforced polymer

Compressive strength concrete cylinder (f'_{c0})	47 Mpa
Thickness of carbon fiber (t)	0.117mm
Elasticity modulus of CFRP (E_{frp})	208760 Mpa
Radius of concrete cylinder (R)	75mm
Rupture strain of single layer CFRP($\varepsilon_{h,rup}$)	0.012
Rupture strain of double layer CFRP ($\varepsilon_{h,rup}$)	0.0141
Ultimate axial strain of unconfined concrete (ε_{c0})	0.002
Tensile strength of composite (f_{com})	2500 MPa

Table 5: Input data used in the models for glass fiber reinforced polymer

Compressive strength concrete cylinder (f'_{c0})	47 MPa
Thickness of carbon fiber (t)	0.342mm
Elasticity modulus of GFRP (E_{frp})	75042 MPa
Radius of concrete cylinder (R)	75mm
Rupture strain of single layer GFRP ($\varepsilon_{h,rup}$)	0.011
Rupture strain of double layer GFRP ($\varepsilon_{h,rup}$)	0.012
Poison ratio of concrete	0.2
Tensile strength of composite (f_{com})	830 MPa
Ultimate axial strain of unconfined concrete (ε_{c0})	0.002

and **3** it can be seen that, error in prediction of compressive strength of concrete cylinders confined by carbon fiber using this model was 12% for single layer and 9% for double layer. In case of cylinders wrapped with single layer glass fiber error in prediction of ultimate stress was 10% and for double layer it was 18%. **Fig 12(d)** shows the discrepancy in the model, as well as how the model compares with the experimental data. From inspection of the model prediction it appears that there is a problem with the shape and smoothness of the transition between the first and second branch. From initially inspecting **Fig 12(d)**, it would appear that if there were a line connecting the transition point to the ultimate point, the second branch of the stress-strain diagram would seamlessly join the first and second branches. This would make the second branch nearly tangent to the end of the first branch.

The comparison of the predicted stress-strain curve by proposed model with the test data is shown in **Fig 12**. There is good correlation with the model and the test data. Performance of this model against the present test results are shown in **Fig 13**.

From **Table 2** and **3** it can be seen that, error in prediction of compressive strength

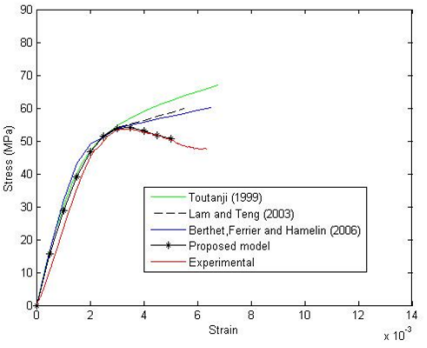

12(a) Single layer CFRP

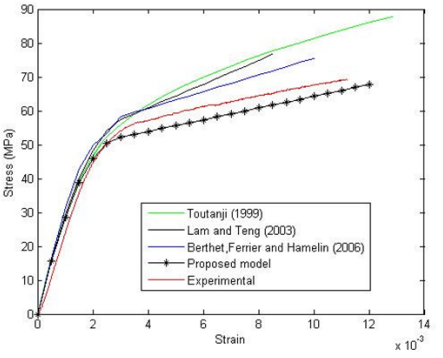

12(b) Double layer CFRP

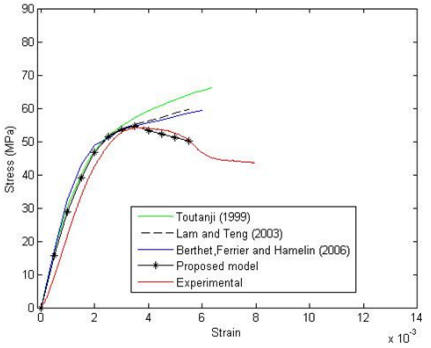

12(c) Single layer GFRP

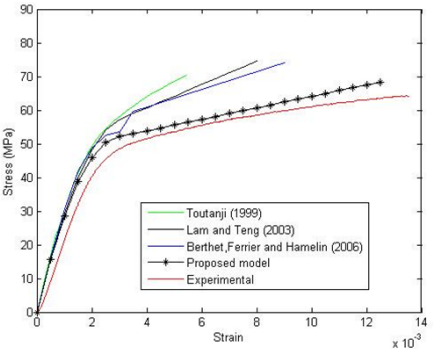

12(d) Double layer GFRP

Figure 12: Comparison of the predicted stress-strain curves with the actual test data.

of concrete cylinders confined by carbon fiber using this model was 0.8% for single layer and 2% for double layer. In case of cylinders wrapped with single layer glass fiber error in prediction of ultimate stress was 0.5% and for double layer it was 6%. Using this model error in prediction of compressive strength was less than 10 % for concrete cylinders wrapped with carbon or glass fiber reinforced polymer for single and double layer. Error in prediction of ultimate strain was 19% for one layer CFRP cylinders, 8% for two layers CFRP cylinders. In case of cylinders wrapped with single layer glass fiber error in prediction of ultimate strain was 33% and for double layer it was 5%. Totally, a good correlation between the model and the test data was observed using proposed model comparative with other models.

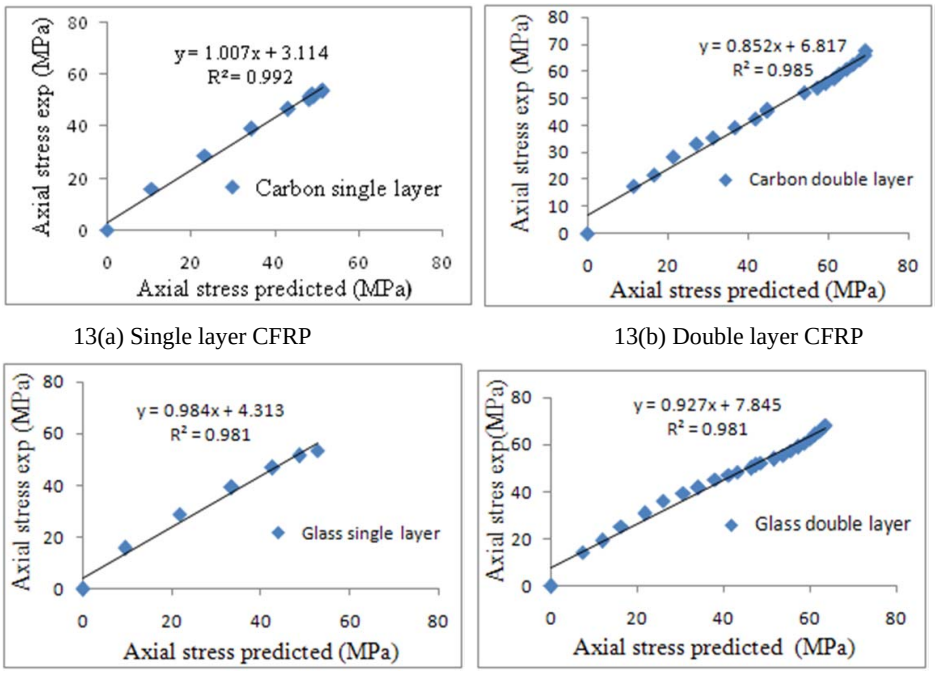

13(a) Single layer CFRP

13(b) Double layer CFRP

13(c) Single layer GFRP

13(d) Double layer GFRP

Figure 13: Performance of the proposed model against the present test results

4 Conclusions

This paper presents results of experimental and analytical investigations of CFRP and GFRP confined specimens. Concrete cylinders have been confined with CFRP and GFRP wrapping. It is observed that the stress-strain curve for concrete confined by FRP composites behaves bilinearly. The first portion of the stress-strain curve traces that of unconfined concrete until the FRP wrap start to get activated. The increase in the peak load was aproximately by 10 percent for concrete cylinders wrapped with single layer carbon or glass FRP, with addition of second layer, increased the peak load by 30 percent for carbon fibre and by 40 percent for glass fibre when compared to the unconfined concrete.Tension test has been conducted on CFRP and GFRP coupons and it is observed that stress-strain curve of FRP cupons was linear up-to failure load. The maximum strain at failure was well beyond 0.011 for both carbon and glass FRP coupons. A detailed review of analytical model for predicting stress-strain relationship has been carried out and a new model has been proposed and validated with experimental results. A good correlation between the

proposed model and the test data was observed. The relationship can quite well predict the ultimate axial strains and stresses and reproduce finely the stress–strain response of confined concrete with carbon or glass FRP.

Acknowledgement: Authors thank ARC Murthy, J.Rajasankar and J.K.Dattatreya Scientists for the discussions during the study.This paper is being published with kind permission of the Director, CSIR-Structural Engineering Research Centre (SERC) Chennai. Authors gratefully acknowledge the support of technical staff at Advanced Materials Laboratory (AML) - SERC, Chennai during the experimental work.

5 Refferences

Ahmad, S. H.; Shah, S.P. (1982): Stress-strain curves of concrete confined by spiral reinforcement. *ACI Journal*, vol.79, no.6, pp.484-490.

Berthet, J.F.; Ferrier, E.; and Hamelin, P. (2006): Compressive behavior of concrete externally confined by composite jackets Part B: Modeling. *Construction and Building Materials*, vol. 20, no. 5, pp. 338-347.

Cusson, D.; Paultre, P. (1995): Stress-strain model for confined high strength concrete. *J. Struct. Engrg., ASCE*, vol.121, no.3, pp.468-477.

Fardis M. N; Khalili H.(1982): FRP encased concrete as a structural material. *Magazine of concrete Research*, vol. 34, no.122, pp: 191-202.

Karbhari, V.M; Gao.Y (1997): Composite Jacketed Concrete under Uniaxial Compression- Verification of Simple Design Equations. *Journal of Materials in Civil Engineering*, vol.9, no.4, pp: 185-193.

Lam. L; Teng. J.G (2003): Design – Oriented stress – strain model for FRP-confined concrete. *Construction and Building Materials*, Vol. 17, pp: 471- 489.

Mander J. B; Priestly M.J.N; Park R (1988): Theoretical stress-strain model for confined concrete. *Journal of Structural Engineering*, ASCE, vol.114, no.8, pp. 1804- 1826.

Mirmiran A; Shahawy M. (1996): A new concrete filled hollow FRP composite column. *Composites: part B; 27 B*, Elsevier, pp. 263-268.

Nanni A; Bradford N.M. (1995): FRP jacketed concrete under uniaxial compression. *Construction and Building Materials*, vol. 9, no.2; pp. 115-124.

Newman, K.; Newman, J.B. (1972): Failure Theories and Design Criteria for Plain Concrete. Proceedings, International Civil Engineering Materials Conference on Structure, *Solid Mechanics and Engineering Design* (Southampton, 1969), Wiley Interscience, New York, Part 2, pp. 963-995.

Richard R.M.; Abbott B.J. (1975): Versatile elastic–plastic stress strain formula. *J Eng Mech Div*, vol.101, no.4, pp.511-515.

Richart, F.E.; Brandtzaeg, A.; and Brown, R. L. (1928): A study of failure of concrete under combined compressive stresses. Bulletin No.185. Univ. of Illinois, Engineering Experimental Station, Urbana, III.

Toutanji H. A. (1999): Stress-strain characteristics of concrete columns externally confined with advanced fiber composite sheets. *ACI Materials Journal*, vol. 96, no. 3, pp. 397-404

Xiao Y.; Wu H. (2000): Compressive behavior of concrete confined by carbon fiber composite jackets. *J Mater Civ Eng,* ASCE, vol.12. no.2, pp.139 –46.